



HAL
open science

Multistage Optimization of a Petroleum Production System with Material Balance Model

Cyrille Vessaire, Jean-Philippe Chancelier, Michel de Lara, Pierre Carpentier, Alejandro Rodríguez-Martínez, Anna Robert

► **To cite this version:**

Cyrille Vessaire, Jean-Philippe Chancelier, Michel de Lara, Pierre Carpentier, Alejandro Rodríguez-Martínez, et al.. Multistage Optimization of a Petroleum Production System with Material Balance Model. Computers & Chemical Engineering, 2022, 167, pp.108005. 10.1016/j.compchemeng.2022.108005 . hal-03508607v2

HAL Id: hal-03508607

<https://hal.science/hal-03508607v2>

Submitted on 19 Sep 2022

HAL is a multi-disciplinary open access archive for the deposit and dissemination of scientific research documents, whether they are published or not. The documents may come from teaching and research institutions in France or abroad, or from public or private research centers.

L'archive ouverte pluridisciplinaire **HAL**, est destinée au dépôt et à la diffusion de documents scientifiques de niveau recherche, publiés ou non, émanant des établissements d'enseignement et de recherche français ou étrangers, des laboratoires publics ou privés.

Multistage Optimization of a Petroleum Production System with Material Balance Model

Cyrille Vessaire*, Jean-Philippe Chancelier*, Michel De Lara*,
Pierre Carpentier†, Alejandro Rodríguez-Martínez‡, Anna Robert§

September 19, 2022

Abstract

In this paper, we propose a mathematical formulation for the optimal management over time of an oil production network as a multistage optimization problem. The proposed model differs from common practice where the reservoir of the oil production network is approximated by decline curves or by black-box simulators. We model the reservoir as a controlled (non-linear) dynamical system by using material balance equations, under the standard assumptions that the fluids follow a black-oil model and that the reservoir has a tank-like behavior. The state of the dynamical system has five dimensions: the total volume of respectively oil, gas, and water in the reservoir; the total pore volume; and the reservoir pressure. We use a dynamic programming algorithm to numerically solve the multistage optimization problem on two specific instances of the general optimization problem where the state dimension can be reduced from dimension five to dimension one or two. More precisely, the first numerical application consists in optimizing the production of a dry gas reservoir which is subdivided in two tanks and which leads to a two-dimensional state (one dimension per tank), whereas the second numerical application tackles an oil reservoir with water injection which leads to a two-dimensional state. The two applications illustrate that our approach handles interconnected tanks (in the dry gas case) and that our approach allows optimization beyond first recovery of oil (in the oil with water injection case). We also provide numerical and theoretical comparisons with decline curves in the dry gas application.

1 Introduction

Oil and gas projects usually span over several decades and involve complex planning and decision-making. Therefore, multistage optimization is a relevant tool to address the long-term performance of such projects. This is the focus of this paper.

The lifetime of a field usually consists of five phases: exploration, where reservoirs containing hydrocarbon are found; appraisal, to give a value to a field; development, where infrastructures are planned and installed; production, where hydrocarbon is finally produced; abandonment, where the field stops producing and infrastructures are decommissioned and removed. In this paper, we focus on the production phase. We consider that the infrastructure has already been installed in the development phase, and we thus focus on finding a production schedule that maximizes the profit over the full production phase.

Now, we position our contribution with respect to the currently available literature. According to the survey (Khor et al., 2017), there is extensive research on how to optimize the production phase, with multiple approaches. The authors present three main methods for the optimization of petroleum production systems: sensitivity analysis by employing simulation tools, heuristic rules and mathematical optimization, the approach of this paper. Most of the literature resorts to the first two approaches.

Regarding mathematical optimization, most works on the topic have considered black-box simulators to describe the reservoir dynamics: Hegguler et al. (1997) consider integrating both a network model

*CERMICS, Ecole des Ponts, Marne-la-Vallée, France

†UMA, ENSTA Paris, Institut Polytechnique de Paris, Palaiseau, France

‡IAM, TotalEnergies SE, Pau, France

§OneTech/R&D, TotalEnergies SE, Saclay, France

and a proprietary reservoir model (a commercial simulation software for reservoir modeling); Gerogiorgis et al. (2006) combine a proprietary reservoir simulator with a general optimization formulation. In Sarma et al. (2006) a closed-loop multistage optimal control approach with a simulator that can be updated with new data from sensors is considered. It is also a standard practice to add some optimization layer over a commercial reservoir simulator to locally improve a production planning, such as modifying the pressure on different points of the petroleum production system to locally improve an operational solution (see ECLIPSE by Schlumberger, or GAP and MBAL by Petroleum Experts). In theory, such approach could be amenable to dynamic programming. However, this is not done in practice due to the the computation time of a single simulation run.

A limited fraction of the literature addresses the problem as a multistage optimization problem, such as in Iyer et al. (1998); Gupta and Grossmann (2012); Marmier et al. (2019). In those papers, the formulation relies on dynamical models based on decline curves (or type curves). In short, decline curves are functions that take as input the cumulative production and return the maximal well rate. In the context of mathematical optimization, decline curves were first assumed to be linear, such as in Bohannon (1970), before being assumed to be piecewise linear in Frair and Devine (1975) or polynomial in Marmier et al. (2019), or even being assumed to be given by a set of logical relationships for shale gas in Hong et al. (2020), when algorithms could treat those refinements. The decline curves are generally constructed by using a foresight of the optimal solution that is looked after, as they are usually generated by assuming a production schedule. In Satter and Iqbal (2016), the authors write that, usually, decline curves analysis is performed under one key assumption: the wells produce at “constant bottom-hole pressure”. They also state that “in reality, such a condition may not be observed”. Note that decline curves can, in some cases, provide an accurate representation of the reservoir if the wells that constitute the oil field are independent of each other, and when we are only considering first recovery of oil and gas (i.e. when we are only producing fluids in the reservoir and without any injection of gas and water in the reservoir). Despite those shortcomings, mathematical formulations using decline curves are commonly used in oilfield development studies. For example, two case studies, one in Brazil (Silva and Guedes Soares, 2021) and one in New Mexico (Davis, 2021) use decline curves to solve a multistage optimization problem.

Part of the literature also tries to develop a middle ground between using a black-box reservoir simulator and using decline curves. For example, some papers use parametrized surrogate models (also called proxy models). Parameters of the surrogate model are to be adjusted to fit simulators output or real data (see (Caballero and Grossmann, 2008)). Numerous applications following the methodology developed in Caballero and Grossmann (2008) have been done, each one being characterized by a specific surrogate model: in Lei et al. (2022), a proxy model (presented in Lei et al. (2021)) that takes into account the decommission timing and costs in the development planning is used; whereas in Camponogara et al. (2017), the authors use MILP as a proxy model and apply it to a case in the Santos Basin; finally, in Moolya et al. (2022), the authors also use a MILP surrogate model combined with aggregation and disaggregation methods in well placement problems. In Epelle and Gerogiorgis (2020), the authors compare the performances between MILP and MINLP formulations of the surrogate model.

In this paper, we represent the reservoir as a controlled dynamical system based on black-oil model and conservation laws (mass balance equations) for a tank-like reservoir instead of using decline curves or surrogate models based on a reservoir simulator. Mass balance equations belong nowadays to the folklore of petroleum engineering and have been described many times in the reservoir modeling literature (see Dake (1983)). We formulate the management problem as a multistage optimization problem, and we use the dynamic programming algorithm to solve it (see Bertsekas (2016)). To the best of our knowledge, this approach is new in the oil and gas literature. This formulation is well adapted to first and secondary recovery of oil and gas cases. Moreover, multistage optimization and dynamic programming are well adapted to tackle more complex formulations with uncertain parameters and partial observations.

2 Formulation of the management of a petroleum production system as a multistage optimization problem

We consider a production system composed of a reservoir and production assets (pipes, wells, chokes). We represent the topology of the production assets as a simple graph $\mathcal{G} = (\mathbb{V}, \mathbb{E})$, where \mathbb{V} is the set of vertices and $\mathbb{E} \subset \mathbb{V}^2$ is the set of edges. Controls are variables indexed by either vertices or edges. We place the different production assets on the graph, with the pipes as the edges of the graph, and the

rest of the assets, such as the well-heads, positioned on the vertices of the graph. This is illustrated in Figure 1. The wells' perforations are represented as vertices (w_i in Figure 1) where the fluids produced enter the graph. On the other vertices, we have assets such as the well-head chokes (wh_i in Figure 1), or joints between different pipes (noted i_1). We can also have valves to open or close pipes. Finally, we have an export point (on the vertex e).

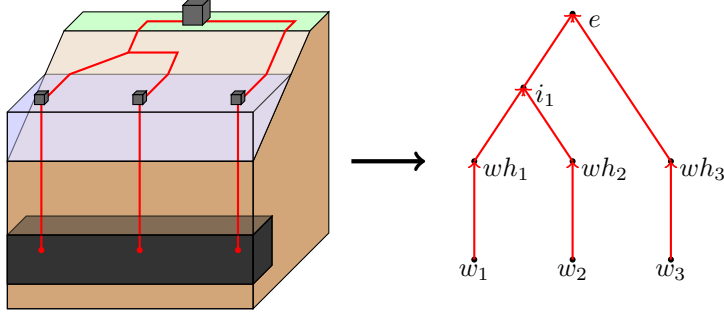


Figure 1: Representing a production network as a graph

All the relevant operational constraints and features - such as pressure loss on the pipes, mass balance of the fluids at each vertex, allowed pressures, and flow rate ranges in the different assets or unavailability due to maintenance - are modeled as constraints using variables defined on the edges and vertices of the graph. Indeed, the graph allows us to define the different controls we can apply to the system, such as opening or closing valves or changing the well-head pressures. Detailed formulations on the production network can be seen in (Gupta and Grossmann, 2012). We will not explicit it in the general case as this is not our main focus, and we only present numerical applications without taking into account the production network.

As we aim to optimize the system over the whole production phase (i.e. over multiple years), we consider multiple time steps belonging to a finite set $\mathbb{T} = \{0, 1, 2, \dots, T\}$ where the parameter T is a natural number. Those time steps are usually monthly¹, but under certain conditions other time steps may be considered.

We propose (and are going to detail) a general formulation of the petroleum production system optimization problem as follows

$$\mathcal{J}^*(x_0) = \max_{x,u} \sum_{t=0}^{T-1} \rho^t \mathcal{L}_t(x_t, u_t) + \rho^T \mathcal{K}(x_T) \quad (1a)$$

$$s.t. \quad x_0 \text{ given}, \quad (1b)$$

$$x_{t+1} = f(x_t, u_t), \quad \forall t \in \mathbb{T} \setminus \{T\}, \quad (1c)$$

$$u_t \in \mathcal{U}_t^{ad}(x_t), \quad \forall t \in \mathbb{T} \setminus \{T\}. \quad (1d)$$

The variables in Problem (1) are: *i*) the state of the reservoir $x_t \in \mathbb{X} \subset \mathbb{R}^n$ (with \mathbb{X} the state space); *ii*) the controls $u_t \in \mathbb{U} \subset \mathbb{R}^p$ (with \mathbb{U} the control space), which are the decisions that can be taken at time step t (for example, the pressure $P_{v,t}$ at the different vertices $v \in \mathbb{V}$ of the graph, and the Boolean $o_{e,t}$ stating if a pipe $e \in \mathbb{E}$ of the graph is opened or closed). The reservoir is defined as a controlled dynamical system, with state x_t , control u_t and an evolution function f of the controlled dynamical system, whose construction is the focus of Section 3. At every time step t , when the decision maker takes decision u_t , an instantaneous gain denoted by $\mathcal{L}_t(x_t, u_t)$ occurs. In the last stage, the final state x_T is valued as $\mathcal{K}(x_T)$. We denote by ρ the discount factor. We finally obtain the objective function seen to the right of the max in Equation (1a) by adding all terms. The known initial state of the reservoir is defined in Equation (1b). The controlled dynamics of the reservoir is given in Equation (1c). Equation (1d) states that, at each time step t , the allowed controls belong to an admissibility set that depends on x_t . The dependence is noted by $\mathcal{U}_t^{ad}(x_t)$, which is for each time step t a set-valued mapping that takes a given state x_t of the reservoir and returns the set of allowed controls. As far as the petroleum application is concerned,

¹Numerical applications will be done with monthly time steps and a horizon T of 15 or 20 years

the admissibility set notably depends on the reservoir pressure, which constrains the different pressures in the petroleum production system. It also depends on the production network itself: some pipes can be controlled, while others cannot; facilities have planned or unplanned downtimes, etc. Extensive formulations of the admissibility set of the production depending on the reservoir pressure can be seen in [Iyer et al. \(1998\)](#).

The petroleum production system optimization problem, as formulated in (1), is a classical deterministic discrete time optimal control problem. It is known that this problem can be solved by dynamic programming and that the resulting optimal control at time t is a function of the current state at time t .

In order to solve Problem (1), we use a family of value functions $\mathcal{J}_t : \mathbb{X} \mapsto \mathbb{R}$, where we recall that \mathbb{X} is the state space. We call *policy* $\mu = \{\mu_0, \dots, \mu_{T-1}\}$ a set of mappings $\mu_t : \mathbb{X} \rightarrow \mathbb{U}$ from states x into admissible controls u . We have the following proposition (see ([Bertsekas, 2016](#), Chap. 1)).

Proposition 1. *For every initial state $x_0 \in \mathbb{X}$, the optimal cost $\mathcal{J}^*(x_0)$ of Problem (1) is equal to $\mathcal{J}_0(x_0)$, given by the last step of the following algorithm, which proceeds backward in time from final time step T to initial time step 0:*

$$\mathcal{J}_T(x) = \rho^T \mathcal{K}(x), \quad \forall x \in \mathbb{X}, \quad (2a)$$

$$\mathcal{J}_t(x) = \max_{u \in \mathcal{U}_t^a(x)} \left(\rho^t \mathcal{L}_t(x, u) + \mathcal{J}_{t+1}(f(x, u)) \right), \quad \forall x \in \mathbb{X}, \forall t \in \mathbb{T} \setminus \{T\}. \quad (2b)$$

Furthermore, if $u^* = \mu_t^*(x)$ maximizes the right-hand side of (2b) for each x and t , then the policy $\mu^* = \{\mu_0^*, \dots, \mu_{T-1}^*\}$ is optimal.

To solve Problem (1), we compute \mathcal{J}_0 . To do so, we use a dynamic programming algorithm (see Algorithm 1). For that purpose, we discretize the controls, that now belong to a finite set denoted by \mathbb{U}_d , and the states that belong to a finite set \mathbb{X}_d . Numerically, we also use a multi-linear interpolation for the value functions between the states.

Algorithm 1: dynamic programming algorithm used to solve Problem (1)

```

for  $x \in \mathbb{X}_d$  do
   $\mathcal{J}_T(x) = \rho^T \mathcal{K}(x);$ 
for  $t = T - 1, \dots, 1$  do
  for  $x \in \mathbb{X}_d$  do
    best_value =  $-\infty$ ;
    best_controls = 0;
    for  $u \in \mathbb{U}_d$  do
      current_value =  $\rho^t \mathcal{L}_t(x, u) + \mathcal{J}_{t+1}(f(x, u));$ 
      if current_value  $\geq$  best_value then
        best_value = current_value;
        best_controls =  $u$ ;
     $\mathcal{J}_t(x) =$ best_value;
     $\mu_t(x) =$ best_controls;
  return  $(\mathcal{J}_t, \mu_t)_{t \in \mathbb{T}}$ 

```

3 Formulation of the reservoir extraction as a controlled dynamical system

In this section, we show how to represent the time evolution of the reservoir as a dynamical system, that is, involving a state x , a control u and an evolution function f such that, for each time step t , we

have $x_{t+1} = f(x_t, u_t)$. It is shown in Appendix A that a possible state - which is the one we henceforth consider, for modeling the reservoir when using the black-oil model and conservation laws for a tank-like reservoir - is the 5-dimensional vector $x_t = (V_t^O, V_t^G, V_t^W, V_t^P, P_t^R)$. Its components are defined in Table 1, where Sm^3 stands for standard cubic meter (the volume taken by a fluid at standard pressure and temperature condition: 1.01325 Bara and 15°C), and Bara stands for absolute pressure in Bar.

Symbol	Definition
V_t^O	Amount of oil in the reservoir (Sm^3) at time t
V_t^G	Amount of free gas in the reservoir (Sm^3) at time t
V_t^W	Amount of water in the reservoir (Sm^3) at time t
V_t^P	Total pore volume of the reservoir (m^3) at time t
P_t^R	Reservoir pressure (Bara) at time t

Table 1: Definition of the components of the state

More precisely, to obtain the evolution function f of the content of the reservoir between time t and $t + 1$, we compute the amounts of fluids (oil, gas, water) produced during the period $[t, t + 1[$. We denote them by (F_t^O, F_t^G, F_t^W) and they are described in Table 2. We obtain the production values with a mapping $\Phi = (\Phi^{(1)}, \Phi^{(2)}, \Phi^{(3)}) : \mathbb{X} \times \mathbb{U} \rightarrow \mathbb{R}^3$ such that $(F_t^O, F_t^G, F_t^W) = \Phi(x, u)$. The production mapping Φ depends on the form and specifications of the production network. We present two examples of such Φ in the numerical applications of Section 4, with details in Appendix A.

Symbol	Definition
F_t^O	Volume of oil produced (Sm^3) during $[t, t + 1[$
F_t^G	Volume of gas produced (Sm^3) during $[t, t + 1[$
F_t^W	Volume of water produced (Sm^3) during $[t, t + 1[$

Table 2: Definition of the productions

We make the following assumptions on the reservoir (as formulated in Dake (1983)): first, the fluids contained in the reservoir follow a *black-oil* model; second, we consider that we have a tank-like reservoir. Thanks to those two standards assumptions, we can formulate the reservoir and the production system as a controlled dynamical system.

Proposition 2. *There exists a function $\Xi : \mathbb{X} \times \mathbb{U} \rightarrow \mathbb{R}$ such that the following function $f : \mathbb{X} \times \mathbb{U} \rightarrow \mathbb{R}^5$*

$$f : (x, u) \mapsto \begin{pmatrix} x^{(1)} - \Phi^{(1)}(x, u) \\ x^{(2)} - \Phi^{(2)}(x, u) + \left[x^{(1)} R_s(x^{(5)}) - (x^{(1)} - \Phi^{(1)}(x, u)) R_s(\Xi(x, u)) \right] \\ x^{(3)} - \Phi^{(3)}(x, u) \\ x^{(4)} (1 + c_f(\Xi(x, u) - x^{(5)})) \\ \Xi(x, u) \end{pmatrix} \quad (3)$$

is the dynamics of the reservoir in (1c) (with $x = (x^{(1)}, \dots, x^{(5)})$, R_s a given function of the reservoir pressure called the solution gas function, and c_f a given parameter called the pore compressibility of the reservoir).

Proof. See Appendix A. □

4 Two numerical applications

We now present two numerical applications that illustrate how the material balance formulation can be used. The numerical applications are done on simple reservoirs. In §4.1, the first application is a gas reservoir that can be modeled with two tanks and with a connection, of known transmissivity, linking them together. It illustrates how the formulation can be applied to complex cases with multiple tanks.

In §4.2, the second application we consider is an oil reservoir where pressure is kept constant through water injection. This shows how we can take into account injection to go beyond the first recovery of oil and gas. All numerical applications were performed on a computer equipped with a Core i7-4700K and 16 GB of memory.

4.1 A gas reservoir with one well

In the first application, we consider a real gas reservoir, for which production data are available. The recorded data come from a field approaching abandonment. We only considered a sub-field of a much larger field, the sub-field being constituted of an isolated reservoir with one well.

Our goal here is to show how simple cases can be tackled with the material balance formulation, and that the formulation can also be applied to cases with multiple tanks. We first present a state reduction of this case. We then present a model with one tank, and then a model with two tanks, mimicking an evolutive construction of the reservoir model. Indeed, when optimizing a real petroleum production system, the models are improved as data are analyzed. Hence, reservoir models will get more complex to fit the gathered exploitation data, such as going from a one tank model to a two tanks model. We therefore present the models following such timetable, going from a cruder to a more refined reservoir model.

Characteristics of the case. The geology of this particular sub-field makes it perfect for a tank model, as proved by many years of perfectly matched production. Also, the simplicity of the fluids with a high methane purity makes the black-oil model a very realistic assumption. The reservoir can be modeled with either one or two tanks, while the well’s perforations are modeled with a known stationary inflow performance relationship, noted IPR^G . The two tanks model is illustrated in Figure 2. We do not consider the rest of the network, so that we will not have to take into account any vertical lift performance (VLP) necessary to lift oil to the surface. This implies that the only control we consider is the bottom hole flowing pressure (BHFP), P_t , resulting in the problem known as *optimization at the bottom of the well*. We hence assume that there is no “pipe” necessary to move gas from the reservoir to the surface, thus assuming that the network is only constituted of the well-perforations which allow the production of gas. Indeed, optimizing with the bottom hole flowing pressure makes it easier to compare the different reservoir models, as we directly act on the reservoir. Adding the vertical lift performance only adds a layer of complexity to the comparison of the models, while the only benefit would be to get results closer to an actual field production. All in all, adding the vertical lift performance only adds more constraints on the mathematical formulation and may mask the impact of the reservoir model. As the focus of this paper is to present a formulation with a new reservoir model, we decided not to take into account the vertical lift performance. We also did not try to go beyond the two tanks model.

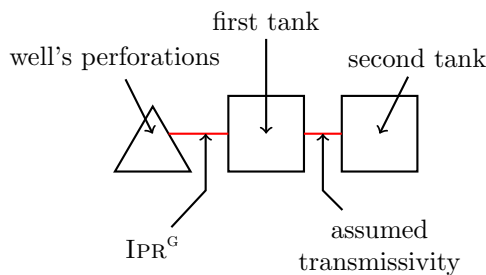


Figure 2: Representation of the two tanks model

Formulation and state reduction. In this first application, we consider a reservoir that contains only gas and water. We first assume that we only produce some gas, and that no fluids are re-injected in the reservoir. Moreover, we assume that there is no water production, and thus the amount of water remains stationary. Therefore, $V_t^W = V_0^W$ for all $t \in \mathbb{T}$, the initial amount of water V_0^W being known. We therefore only need to consider the evolution of the amount of gas, the pressure and the total pore

volume as states variables. As shown in Appendix B, we can further reduce the state, and we only need to consider the amount of gas in the reservoir as the reservoir state. Since we do an optimization at the bottom of the well, we only have one control to consider, the bottom-hole flowing pressure, noted P_t . We therefore have state $x_t = V_t^G$ and control $u_t = P_t$.

The optimization problem we consider here is to maximize the revenue of the gas production. At each time t , we sell gas at price r_t , with a discount factor ρ . The general optimization problem (1) after state and control reduction when considering the gas reservoir and one tank is given by

$$\max_{(V_t^G, P_t, P_t^R, F_t^G)} \sum_{t=0}^{T-1} \rho^t r_t F_t^G \quad (4a)$$

$$s.t. \quad V_0^G = x_0, \quad (4b)$$

$$P_t^R = \Psi_{1T}(V_t^G), \quad \forall t \in \mathbb{T}, \quad (4c)$$

$$F_t^G = \frac{\text{IPR}^G(P_t^R - P_t)}{B_G(P_t^R)}, \quad \forall t \in \mathbb{T} \setminus \{T\}, \quad (4d)$$

$$V_{t+1}^G = V_t^G - F_t^G, \quad \forall t \in \mathbb{T} \setminus \{T\}, \quad (4e)$$

$$F_t^G \geq 0, \quad \forall t \in \mathbb{T} \setminus \{T\}, \quad (4f)$$

$$V_t^G \geq 0, \quad \forall t \in \mathbb{T}, \quad (4g)$$

$$P_t \geq 0, \quad \forall t \in \mathbb{T} \setminus \{T\}, \quad (4h)$$

as detailed in Appendix B.

4.1.1 One tank gas reservoir model

Fitting model to real data. We use production data from a sector of a real gas field, to check that the reservoir model described with the Constraints (4c) and (4e) accurately follows real measurements on the gas field after fitting the model. More precisely, we apply a given real production schedule on a part of the field (only one well), and check that the pressure we simulate in the reservoir is close to the corresponding measured pressure. The historical production spans over 15 years, and we have monthly values, which is why we consider monthly time steps for Problem (4).

As can be seen in Figure 3, the one tank model fits the observation. However, there is a gap between the simulated and measured pressures whose relative value may exceed 10%. Since the simulated pressure tends to be higher on the first half of the production, we start by underestimating the decline of the production. Then, during the second half of the production, the simulated pressure is lower than the measured pressure, which means we overestimate the decline of the production. This elastic effect is most likely due to the simplification of removing the secondary tank in the model. Indeed, the secondary tank act as a buffer which reacts slowly, explaining the extra pressure at the beginning and then sustaining a better value of the pressure later on.

Optimization of the production on the one tank approximation. We use dynamic programming (see Algorithm 1) to get an optimal production policy. We consider that the revenue per volume of gas is the historical gas spot price of TTF (Netherlands gas market) from 2006 to 2020, and we do not consider any operational cost.

We now present the results of the one tank model. The results are illustrated in Figures 4 and 5, and summarized in Table 3. We notably remark in Figure 5 that the optimal production stops when prices are low as we fully take advantage of the perfect knowledge of the future prices.

There is a massive increase in the total gains when using the optimal policy, compared to the real production. We also produce far more over the optimization time period (2,850 MSm³ instead of 2,250 MSm³). However, those results are not truly comparable. We do not have access to the criteria used to choose the real production. Optimized and real productions cannot be compared as they do not share the same objective function. Moreover, since the considered case is a small part of a much larger production network, we cannot compare the results to the actual production policy used for fitting the model, which was made with the rest of the network in mind. Furthermore, our optimization is made at the bottom of the well (BHFP). We only take into account the inflow performance of the well, not the vertical lift necessary to bring the gas to the surface. The resulting rates are therefore not fully realistic,

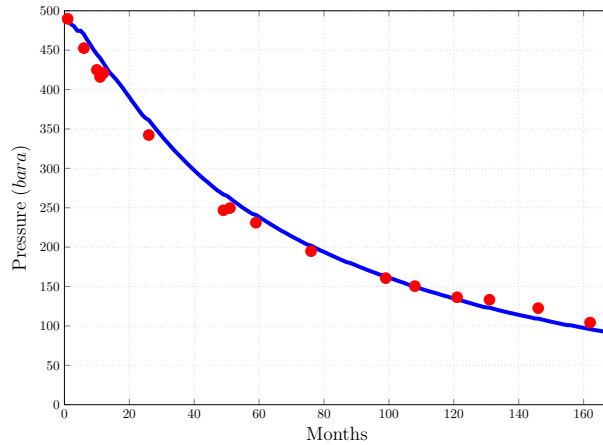


Figure 3: Comparison of the simulated one tank reservoir pressure to the historical measured pressure when applying the same (historical) production schedule. The blue curve is the simulated pressure in the tank, whereas the red dots are the measured pressures.

reaching values closer to a multi-well development. Finally, the historical production was made without knowing future prices, and could also have been made with other constraints to ensure a minimal production of the field, or having a positive cash-flow (constraints due to the field's exploitation contract). While not directly comparable, this gas reservoir application still illustrates one of the best-case scenarios of the dynamic programming approach, and it shows how much could be gained from using a multistage material balance formulation.

Since the dynamic programming algorithm uses a discretization of the state space \mathbb{X}_d and the control space \mathbb{U}_d , we tried different uniform discretizations for the states and controls spaces to prevent any side effects due to the chosen discretization. We do not observe notable changes in the value function past a 10,000 points uniform discretization of the state space and a 20 points discretization of the control space, which are the values we used in this case study. Details on the effect of the discretization can be found in Appendix C.

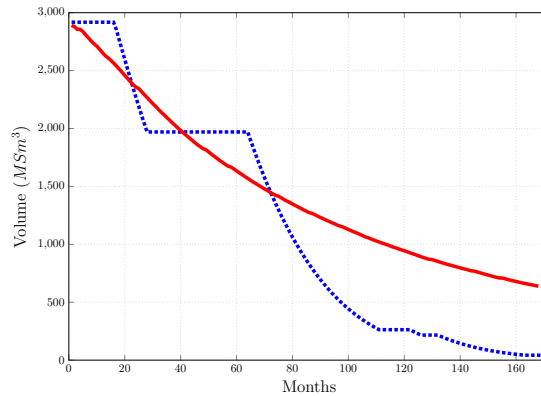


Figure 4: Evolution of the content of the reservoir in the one tank model. The dotted blue curve is the optimal (anticipative) trajectory of the amount of gas, while the red curve is the trajectory with the historical production.

Comparison to policy derived from decline curves. In this paragraph, we compare the material balance formulation to those using decline curves or oil-deliverability curves, such as in [Iyer et al. \(1998\)](#); [Gupta and Grossmann \(2012, 2014\)](#); [Marmier et al. \(2019\)](#). The decline curves formulation and the way to numerically obtain decline curves are given in Appendix D. The following proposition shows that the decline curves formulation is equivalent to the material balance formulation when considering a one-tank

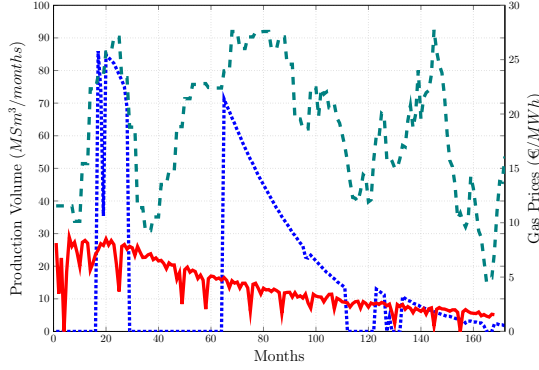


Figure 5: Trajectories of the production. The dotted blue curve is the optimal (anticipative) production in the one tank model, the red one is the historical production, whereas the dashed green curve is the average monthly gas price.

model.

Proposition 3. *The formulation using decline curves, written*

$$\max_u \sum_{t=0}^T \rho^t \mathcal{L}_t(u_t) \quad (5a)$$

$$s.t. \quad F_t^o \leq h \left(\sum_{s=0}^{t-1} F_s^o \right), \quad \forall t \in \mathbb{T} \setminus \{0\} \quad (5b)$$

$$u_t \in \mathcal{U}_t^{ad} \left(\sum_{s=0}^{t-1} F_s^o \right), \quad \forall t \in \mathbb{T}, \quad (5c)$$

is equivalent to the material balance formulation when the state of the reservoir is one-dimensional.

Proof. See Appendix D □

We obtain the decline curve h used in Inequality (5b) by first computing the maximal production value for the same discrete states as the ones used in the dynamic programming approach. Then, piecewise interpolation between the computed values is used to obtain the value of the decline curve everywhere. It is worth noting that, when using piecewise linear approximation for the decline curves, the maximization problem (5) turns out to be a MIP (Mixed Integer Problem) with linear constraints and with more than 170,000 binary variables. We solve that MIP by using the commercial solver Gurobi 9.1. The results are given in Table 3. Since the material balance formulation (4) uses a one-dimensional state, we obtain similar results between the material balance formulation and the formulation using a decline curve in accordance with Proposition 3. The two approaches thus yield similar production policies. Note however that the dynamic programming approach has a lower computation time than a naive implementation of the decline curve formulation. One could decrease the precision on the decline curve formulation, by using fewer points to describe the decline curve. This would improve its computation time. As this is not the focus of this paper, we did not do such refinement of the numerical experiments for the decline curve formulation.

	CPU time (s)	Value (M€)
Material Balance	653	743
Decline Curves	3,882	743

Table 3: Comparison with regards to CPU time and value between the material balance and decline curve formulation for one tank

4.1.2 Two tanks gas reservoir model

Fitting data. We check if the fitted two tanks reservoir model accurately follows real measurement on the gas field. We use the same data as in the one tank case. The two tanks model more accurately fits the observations, as is depicted in Figure 6 (we have a gap of less than 5% for each measured point). Since the two tanks model is closer to the observations, we consider that it is the reference of “truth” when comparing results of the one tank approximation and the two tanks model.

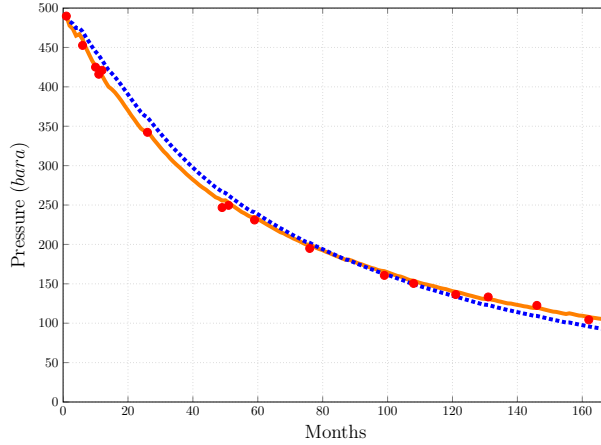


Figure 6: Comparison of the simulated two tanks reservoir pressure to the measured pressure when applying the same production schedule. The blue dotted curve recalls the pressure obtained using the one tank model. The orange continuous curve is the pressure in the first tank obtained using the two tanks model. The red dots are the measured pressure at the bottom of the well.

Optimal production with two tanks. We now present the results of the two tanks model. The only changes compared to the one tank model are on the states and on the dynamics of the reservoir. We use the same prices, and, again, we only do an optimization at the bottom of the well (BHFP). Details on the obtained optimal controls and states trajectory are given in Figure 7 and Figure 8. Once again, we observe that production stops when prices are low, benefiting fully from anticipating the future prices. We also note that more “pauses” are present in the productions when compared to the one tank model (four instead of three). The “pauses” allow the second tank to replenish the first one (see Figure 7). Indeed, production resumes at months 50 to 60, before stopping again for five months. We can then observe that the amount of gas in the first tank is replenished, before we resume production at month 65, at the same date as in the one tank model. We end up producing some more gas than with the one tank model ($2,900 \text{ Sm}^3$ instead of $2,850 \text{ Sm}^3$).

We tried different discretizations for the state space. Notably, using more than 400 possible states per tank and 10 possible controls did not yield any significant improvement in the computed value function. Details on the impact of the discretization are given in Appendix C.

Numerical experiments also reveal that the initial value function \mathcal{J}_0 is almost an affine function of the sum of the states. This seems to imply that the one tank and two tanks model should yield similar results. Such a statement does not hold true, as confirmed by the numerical experiments described in the next paragraph.

Comparing the one tank formulation to the two tanks formulation. To compare the results between the two tanks and one tank formulations, we consider that the two tanks material balance model is the reference. A given sequence of controls $(u_t)_{t \in \mathbb{T} \setminus \{T\}}$ admissible for the one tank model is not necessarily admissible for the two tanks model. Indeed, the admissible control set is given by $\mathcal{U}^{ad}(x_t) = [0, \Psi_{1\mathbf{T}}(x_t)]$ for the one tank model and by $[0, \Psi_{2\mathbf{T}}^{(1)}(x_t^{(1)})]$ for the two tanks model (see Appendix B.1).

Thus, given a sequence of controls $(u_t)_{t \in \mathbb{T} \setminus \{T\}}$ admissible for the one tank model, we produce an admissible sequence of controls for the two tanks model with the use of a *projection* $\Pi_{1\mathbf{T} \rightarrow 2\mathbf{T}} : \mathbb{U}^T \times \mathbb{X} \rightarrow$

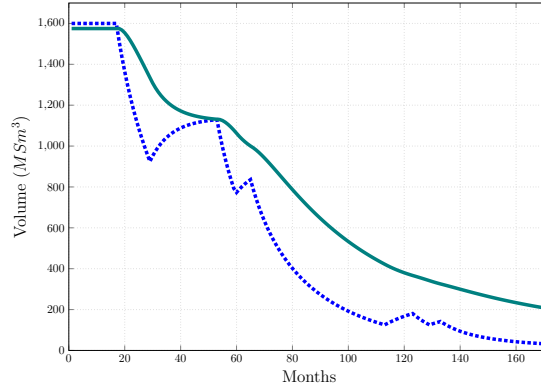


Figure 7: Evolution of the content of the reservoirs when applying the optimal (anticipative) policy in the two tanks model. The dotted blue curve shows the content of the first tank (linked to the well) while the green curve shows the content of the second tank.

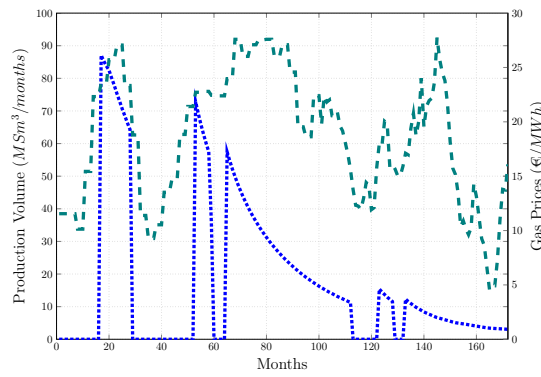


Figure 8: Trajectory of the optimal production in the two tanks model. The dotted blue curve is the optimal (anticipative) production, whereas the dashed green curve is the monthly gas price.

\mathbb{U}^T given as follows. The sequence $(\tilde{u}_t)_{t \in \mathbb{T} \setminus \{T\}} = \Pi_{1\mathbf{T} \rightarrow 2\mathbf{T}}((u_t)_{t \in \mathbb{T} \setminus \{T\}}, x_0)$ is computed recursively for all $t \in \mathbb{T} \setminus \{T\}$ by $\tilde{u}_t = \min \{u_t, \Psi_{2\mathbf{T}}^{(1)}(\tilde{x}_t^{(1)})\}$, where \tilde{x}_t is defined at time 0 by $\tilde{x}_0 = x_0$, and for all $t > 0$ by $\tilde{x}_{t+1} = f_{2\mathbf{T}}(\tilde{x}_t, \tilde{u}_t)$. We can get a sequence of admissible controls for the two tanks model by applying the projection $\Pi_{1\mathbf{T} \rightarrow 2\mathbf{T}}$ on a sequence of admissible controls for the one tank model.

To compare the one tank and two tank models, we project the optimal sequence of controls returned by the dynamic programming algorithm on the one tank formulation thanks to the projection $\Pi_{1\mathbf{T} \rightarrow 2\mathbf{T}}$. As can be seen in Figure 9, the projected sequence of controls differs from the non-projected sequence: the dotted curve, which represents the projected sequence, is below the dashed curve, which represents the optimal sequence for the one tank model.

As depicted in Figures 9 and 10, the production planning given by the one tank optimization problem differs from the production planning given by the two tanks optimization problem. Moreover, the production planning of the one tank model gives lower gains than anticipated, and is worse than the optimal two tanks model planning. The one tank optimization is thus optimistic on the optimal value of the problem when applied with the reference model. Moreover, there is a 5% difference in value between the one tank and two tanks models (a value of 703 M€ for the translated one tank production planning against 736 M€ for the two tanks production planning). This discrepancy illustrates how having a more accurate model of the reservoir can have a substantial impact on the optimal planning, all other things being equal. It also shows that, contrarily to the assumption presented at the end of the previous paragraph (that the two models could yield similar results if the value function only depended on the sum of the states), the optimal value and control cannot be found with a one tank approximation, and the optimal controls and value functions are not functions of the sum of the states.

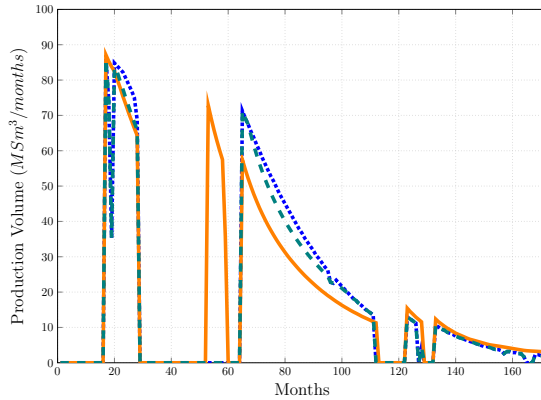


Figure 9: Comparison of the trajectory of the production with the two tanks model as reference. The dotted blue curve is the production planning in the one tank model, the orange curve is for the two tanks model. The dashed green curve is the production planning of the one tank model projected in the two tanks model

Comparison to decline curves with two tanks. We have numerically compared the decline curve and the material balance formulations in a context where they are known to be equivalent, that is, the one tank formulation. We now produce numerical experiments in a context where the equivalence is not assured: two tanks connected with a known transmissibility. We have generated decline curves for the two tanks formulation by following the procedure described in Appendix D. The results returned by the decline curve formulation provide an admissible production in the two tanks model, as it is constrained by an admissible production schedule. We can therefore directly compare the results obtained by the decline curves approach and the two tanks model. The results of the optimization of the two formulations are compiled in Table 4. We end up having close results, with a difference in optimal values of 0.7%, but with a large difference in computing times. However, it appeared that such close results were due to the selected price scenario. Using different prices by randomizing the order in which the different prices appear, the gap between the two approaches widens from 0.5% up to 4%. This implies that the initial price considered was an almost best-case scenario for the decline curves approach. It also shows that the decline curves approach is far less robust to changes in the price data, and that it cannot benefit as

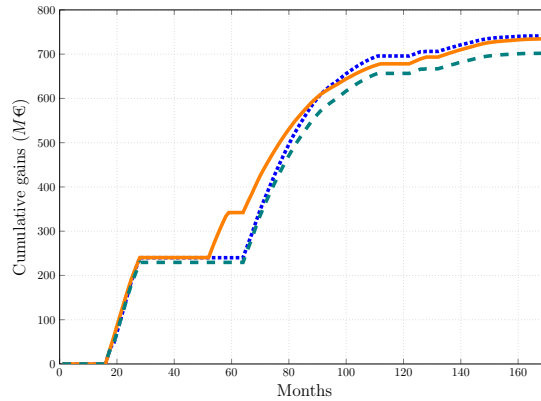


Figure 10: Cumulated gains with the two tanks model as reference. The dotted blue curve is the cumulated gains of the one tank planning in the one tank model, the orange curve is the cumulated gains of the two tanks planning in the two tanks model, and the dashed green curve is the cumulated of the one tank planning projected in the two tanks model

efficiently as the material balance formulation of some effects of the two tanks dynamical system, such as waiting for the second tank to empty itself into the first one.

	CPU time (s)	Value (M€)
Material Balance	706	736
Decline Curves	7,825	731

Table 4: Comparison with regards to CPU time and value between the material balance and decline curve formulation for two tanks with the initial prices sequence.

Overall, this application suggests that the material balance approach can work on complex cases, and that dynamic programming is well suited to optimize an oil field. Moreover, there can be differences with results from the decline curves approach, which are likely to grow larger with the complexity of the system.

4.2 An oil reservoir with water injection

The second application is an oil reservoir with water injection. The goal is to demonstrate how the formulation can be used beyond primary recovery cases, on a numerically simple case. We consider that we have one reservoir which contains both oil and water, produced under pressure maintenance by water injection. Moreover, we consider that the initial pressure is above the bubble-point, which eliminates the possibility of having free gas in the reservoir. This allows us to have once again a one-dimensional state: either the water (which we used for the numerical applications), or the oil in the reservoir. We have $x_t = V_t^w$ and $u = P_t$. Here, we want to maximize the revenue of the oil production. The optimization

problem (1) now becomes

$$\max_{(V_t^w, P_t, w_t^{wc})} \sum_{t=0}^{T-1} \left(\rho^t r_t \alpha \frac{P^R - P_t}{B_o(P^R)} (1 - w_t^{wc}) - \rho^t c_t \alpha \frac{P^R - P_t}{B_w(P^R)} \right) \quad (6a)$$

$$s.t. \quad w_t^{wc} = \text{WCT} \left(\frac{V_t^w B_w(P^R)}{V^p} \right), \quad \forall t \in \mathbb{T}, \quad (6b)$$

$$V_{t+1}^w = V_t^w - \alpha \frac{P^R - P_t}{B_w(P^R)} (w_t^{wc} - 1), \quad \forall t \in \mathbb{T}, \quad (6c)$$

$$F_{min}^w \leq \alpha \frac{P^R - P_t}{B_w(P^R)} (w_t^{wc} - 1) \leq F_{max}^w, \quad \forall t \in \mathbb{T}, \quad (6d)$$

$$F_{min}^o \leq \alpha \frac{P^R - P_t}{B_o(P^R)} (1 - w_t^{wc}) \leq F_{max}^o, \quad \forall t \in \mathbb{T}, \quad (6e)$$

$$P_t \geq 0, \quad \forall t \in \mathbb{T}. \quad (6f)$$

The objective function (Equation (6a)) is divided in two components. At time t , we consider a discount factor ρ and the price r_t of the oil, whereas injecting water costs c_t per cubic meter. The revenue is hence

$$\sum_{t=0}^{T-1} \rho^t (r_t F_t^o - c_t F_t^{wi}).$$

Replacing the produced oil F_t^o and the injected water F_t^{wi} by the relevant functions of the controls (see Equations (29) and (32)) leads to the objective function (6a).

We assume that the water-cut function WCT (the amount of water produced when extracting one cubic meter of liquid at standard conditions) is given by a piecewise linear function. The water-cut depends on the water saturation S^w (proportion of water in the reservoir pore volume). Since the reservoir pressure is kept constant, the total pore volume is constant and the water saturation expression is thus $S_t^w = \frac{V_t^w B_w(P^R)}{V^p}$. This gives us constraint (6b).

Since we want to keep a constant pressure in the reservoir, we need to re-inject enough water to replace the extracted oil. Replacing the oil with water gives a new dynamic for V_t^w as in Equation (6c). Constraints (6d) and (6e) details the oil and water produced depending on the control P_t with their respective bounds. The details of the formulation are given in Appendix B.

We do a monthly optimization, with the historical Brent prices for years 2000–2020 as the prices in the objective function (6a), and a water injection cost of 1 €/m³. Details on the resulting trajectory of the content of the reservoir can be found in Figure 11, whereas details on the production can be found in Figure 12. As previously discussed in §4.1, the optimal policy yields more production when prices are high, and stops producing when they are low. The production goes from one bound to the other (zero production, with $P_t = P^R$, and full production, with $P_t = 0$).

The production also does not fully deplete the reservoir, which means that it is not advantageous to completely deplete the reservoir if one wants to maximize the profit over the optimization time frame (there is still 18.2 MSm³ of oil in the reservoir at time T , as can be seen in Figure 11). Indeed, production slowly diminishes with the volume of oil V_t^o in the reservoir, as can be seen in Figure 12. It is more advantageous to wait for high prices instead of producing, as it would reduce the possible future production. This leads to halting production with some reserves still in the reservoir, as we prefer to wait for a higher price instead of producing when prices are low. As a side effect, numerical experiments reveal that the initial value function \mathcal{J}_0 is almost linear with regards to the state x_0 . However, we only considered simple constraints on the production. As more constraints will be added to the problem, other behaviors will certainly appear. CPU time was 1,575 s for a 100,000 discretization of the state variable, with a value of 3,376 M€. Impact of the discretization can be found in Appendix C.

Overall, this application shows how we can apply the material balance approach beyond first recovery of oil and gas, and that it can be used on different kinds of reservoirs.

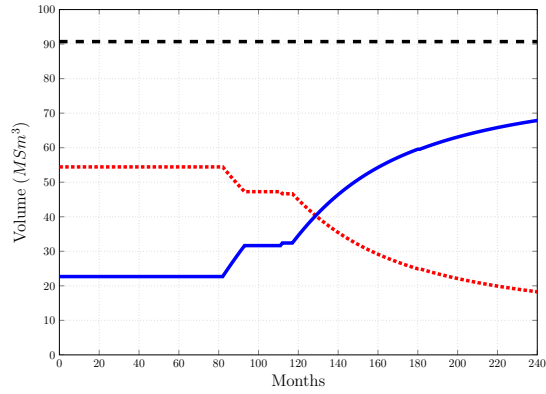


Figure 11: Evolution of the content of the reservoir when applying the optimal policy in the oil reservoir model. The blue curve shows the volume of water in the reservoir, whereas the dotted red curve is the volume of oil the reservoir. The dashed black curve represents the total pore volume

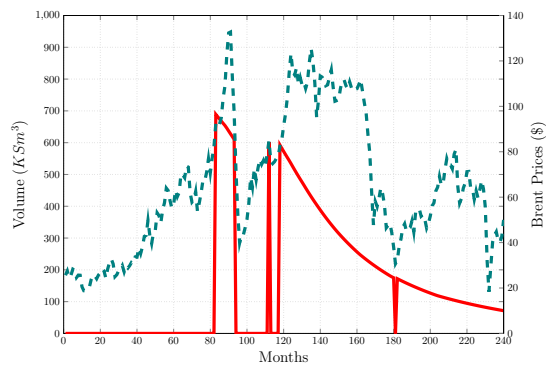


Figure 12: Trajectory of the optimal production in the oil reservoir model. The red curve is the optimal production, whereas the dashed green curve is the monthly oil price

5 Conclusion

In this paper, we have presented a mathematical formulation for the optimal management over time of an oil production network as a multistage optimization problem. In this formulation, the reservoir is modeled as a controlled (non-linear) dynamical system derived from material balance equations and the black-oil model. The state of the derived dynamic system is of dimension five, which is quite large for numerical resolution via dynamic programming algorithm. However, we were able to use Dynamic Programming to numerically solve the management optimization problem for specific cases of interest with either oil or gas, both presenting a reduced dimensionality of the state. We have also shown that our mathematical formulation is an improvement over decline curves formulation. First, as predicted by the theory, we replicated results from decline curve formulations when considering the first recovery of a one tank system (as seen in §4.1.1). Second, in more complex cases with inter-connected tanks, as described in §4.1.2, we have shown that we can surpass the NPV returned by the decline curve formulation. Third, we have gone beyond the first recovery of hydrocarbons, as we have shown in §4.2, where we took into account water injection.

Finally, it is to be noted that the dynamic programming algorithm can be used in a stochastic framework. As an example, we could add uncertainties to the oil and gas prices, instead of assuming that they are known in advance and thus deterministic. Moreover, an even more realistic formulation with *partial observation* of the content of the reservoir could also be explored. Indeed, in oil production systems, the initial state of the reservoir is not known. Such a formulation is amenable to dynamic programming, as will be explored in future works.

Acknowledgements

We would like to thank TEPNL in general and Erik Hornstra in particular for providing data used in this paper.

A Detailed construction of the reservoir as a dynamical system

In this section, we detail the construction of the reservoir as a dynamical system. This serves as the proof of Proposition 2.

A.1 Constitutive equations assuming the black-oil model for the fluids

The black-oil model relies on the assumption that there are at most three *fluids* in the reservoir: oil, gas and water. Moreover, the fluids can be present in the reservoir in up to two phases: a liquid phase, and a gaseous phase. A black-oil representation of a reservoir can be seen in Figure 13. The three fluids, oil, gas and water, can be present in the liquid phase and the gas in the liquid phase is denoted as *dissolved gas*. By contrast, it is assumed that in the gaseous phase, only gas, denoted as *free gas*, can be present.

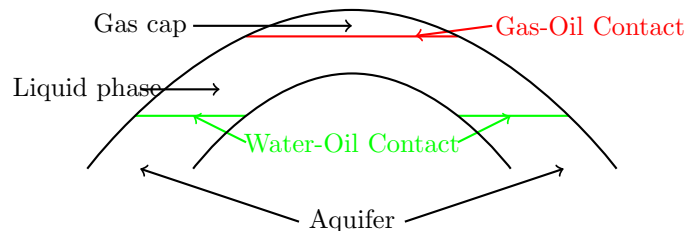


Figure 13: Black-oil Representation of a reservoir

Therefore, in the black-oil model, we consider the following four components

- V^o , the standard volume of oil in the liquid phase,
- V^g , the standard volume of free gas in the gaseous phase,

- V^{DG} , the standard volume of dissolved gas in the liquid phase,
- V^{W} , the standard volume of water in the liquid phase,

where *standard volume* is the volume taken by a fluid at standard pressure and temperature condition (1.01325 Bar and 15°C), also known as stock tank conditions. The units of standard volumes are preceded by a capital S, as in Sm^3 for standard cubic meter.

There are functions in the black-oil model to convert standard volumes into in situ volumes in the reservoir under a given pressure and temperature. The set of functions describing the pressure, volume and temperature behavior of the fluids, under the black-oil assumption, is called the PVT (Pressure-Volume-Temperature) model. We consider here a simplified black-oil model, assuming that the temperature in the reservoir is stationary and uniform, which is a common assumption for a geological formation such as a reservoir. There are four PVT functions, one per component, which are given in Table 5. The PVT functions only depend on the reservoir pressure under the stationary and uniform temperature assumption. As an example, given the oil standard volume, V^{O} , and the reservoir pressure, P^{R} , the oil volume in the reservoir is given by $V^{\text{O}} \times B_{\text{O}}(P^{\text{R}})$.

Notations	Description
B_{O}	Oil formation volume factor. It is the volume in barrels occupied in the reservoir, at the prevailing pressure and temperature, by one stock tank barrel of oil plus its dissolved gas. (unit: <i>rb/stb</i>)
B_{G}	Gas formation volume factor. It is the volume in barrels that one standard cubic foot of gas will occupy as free gas in the reservoir at the prevailing reservoir pressure and temperature. (unit: <i>rb/scf</i>)
B_{W}	Water formation factor. It is the volume occupied in the reservoir by one stock tank barrel of water. (unit: <i>rb/stb</i>)
R_{s}	Solution (or dissolved) gas. It is the number of standard cubic feet of gas which will dissolve in one stock tank barrel of oil when both are taken down to the reservoir at the prevailing reservoir pressure and temperature. (unit: <i>scf/stb</i>)

Table 5: Definition of the PVT functions

One key characteristic of the black-oil model that we use is due to (Danesh, 1998, chap 2), which states that the sum of the physical volumes in the reservoir associated with the three components V^{O} , V^{G} , V^{W} is a decreasing function

$$P^{\text{R}} \mapsto V^{\text{O}} \times B_{\text{O}}(P^{\text{R}}) + V^{\text{G}} \times B_{\text{G}}(P^{\text{R}}) + V^{\text{W}} \times B_{\text{W}}(P^{\text{R}}), \quad (7)$$

of the reservoir pressure.

The last characteristic of the black-oil model concerns the dissolved gas in the oil V^{DG} . It is assumed in Dake (1983) that the standard volume of the dissolved gas V^{DG} is a function of both the standard volume of oil, V^{O} , and the reservoir pressure, P^{R} , as follows

$$V^{\text{DG}} = \delta(V^{\text{O}}, P^{\text{R}}) = V^{\text{O}} \times R_{\text{s}}(P^{\text{R}}). \quad (8)$$

A.2 Conservation law in the reservoir

We assume that the reservoir structural integrity is guaranteed, so there is no leakage of any fluids at any time. We can therefore write mass conservation equations, which are also named *material balance* equations in the oil literature, for each of the four components introduced in §A.1. In order to write the material balance equations of the reservoir, we need to consider the production volumes, F^{O} , F^{G} and F^{W} which are the standard volumes of oil, free gas and water extracted from the reservoir.

Using material balance for the standard volume of oil in the liquid phase, we get

$$V_{t+1}^{\text{O}} = V_t^{\text{O}} - F_t^{\text{O}} \quad \forall t \in \mathbb{T} \setminus \{T\}, \quad (9)$$

and, for the standard volume of water, we get

$$V_{t+1}^{\text{W}} = V_t^{\text{W}} - F_t^{\text{W}} \quad \forall t \in \mathbb{T} \setminus \{T\}. \quad (10)$$

The material balance for gas requires some more developments as it mixes the standard volume of free gas and the standard volume of dissolved gas. As given in §A.1, at any time, $t \in \mathbb{T}$, the standard volume of dissolved gas in the liquid phase V_t^{DG} is given by Equation (8). Therefore, between time t and time $t + 1$, the standard volume of dissolved gas evolves from $V_t^{\text{DG}} = \delta(V_t^{\text{O}}, P_t^{\text{R}})$ to $V_{t+1}^{\text{DG}} = \delta(V_{t+1}^{\text{O}}, P_{t+1}^{\text{R}})$. Hence, the quantity $(V_t^{\text{DG}} - V_{t+1}^{\text{DG}})$ of *liberated* gas must be added to the free gas material balance equation. Thus, for all $t \in \mathbb{T} \setminus \{T\}$, we obtain the following mass conservation equation for the standard volume of free gas

$$\begin{aligned} V_{t+1}^{\text{G}} &= V_t^{\text{G}} - F_t^{\text{G}} + (V_t^{\text{DG}} - V_{t+1}^{\text{DG}}) \\ &= V_t^{\text{G}} - F_t^{\text{G}} + (V_t^{\text{O}} \times R_s(P_t^{\text{R}}) - V_{t+1}^{\text{O}} \times R_s(P_{t+1}^{\text{R}})) \end{aligned} \quad (\text{by (8)})$$

$$= V_t^{\text{G}} - F_t^{\text{G}} + \left(V_t^{\text{O}} \times R_s(P_t^{\text{R}}) - (V_t^{\text{O}} - F_t^{\text{O}}) \times R_s(P_{t+1}^{\text{R}}) \right) \quad (\text{by (9)})$$

$$\begin{aligned} &= V_t^{\text{G}} - F_t^{\text{G}} + \left(V_t^{\text{O}} \times (R_s(P_t^{\text{R}}) - R_s(P_{t+1}^{\text{R}})) \right. \\ &\quad \left. + F_t^{\text{O}} \cdot R_s(P_{t+1}^{\text{R}}) \right). \end{aligned} \quad (11)$$

The last conservation equation is given by a physical volume constraint coming from the fact that all four components of the reservoir are kept in the pores of the reservoir rocks. We note V^{P} the total pore volume of the reservoir. Following Dake (1983) and assuming that the pore compressibility c_f is constant, the total pore volume is a function of the pressure in the reservoir given by

$$V_t^{\text{P}} = V_0 \exp(c_f P_t^{\text{R}}), \quad \forall t \in \mathbb{T}, \quad (12)$$

with V_0 the asymptotic reservoir volume when pressure tends to 0.

A linearized version of Equation (12) proposed in Dake (1983) is

$$\frac{V_{t+1}^{\text{P}} - V_t^{\text{P}}}{V_t^{\text{P}}} = c_f (P_{t+1}^{\text{R}} - P_t^{\text{R}}), \quad \forall t \in \mathbb{T} \setminus \{T\}, \quad (13)$$

and is used to derive the state dynamics of the reservoir.

Now, we consider the *saturations* of the fluids which are the proportions of the available pore volume taken by each of the three fluids in the reservoir. Denoting by S^{O} , S^{G} and S^{W} the saturations of respectively the oil, free gas and water components, we obtain that the sum of the three saturations must be equal to one over time

$$S_t^{\text{O}} + S_t^{\text{G}} + S_t^{\text{W}} = 1, \quad \forall t \in \mathbb{T}. \quad (14)$$

Since, for all $t \in \mathbb{T}$ and $i \in \{\text{O}, \text{G}, \text{W}\}$, we have that

$$S_t^i = \frac{V_t^i \times B_i(P_t^{\text{R}})}{V_t^{\text{P}}},$$

Equation (14) gives

$$V_t^{\text{O}} \times B_{\text{O}}(P_t^{\text{R}}) + V_t^{\text{G}} \times B_{\text{G}}(P_t^{\text{R}}) + V_t^{\text{W}} \times B_{\text{W}}(P_t^{\text{R}}) = V_t^{\text{P}}, \quad \forall t \in \mathbb{T}. \quad (15)$$

A.3 Construction of a production function

The time evolution of the reservoir is driven by the three production volumes, F^{O} , F^{G} and F^{W} which are the standard volumes of oil, free gas and water extracted from the reservoir.

Thus, the three production volumes may appear as possible controls on the reservoir. However, when adding a production network to the reservoir model, the controls to be considered are no longer production volumes, but decisions made upon the production network, such as opening or closing a pipe, choosing the well-head or bottom hole pressure, etc.

In the general case, we can assume that the physical model of the production network leads to a production function $\Phi : \mathbb{X} \times \mathbb{U} \rightarrow \mathbb{R}^3$, which relates the production volumes to the variables of the reservoir $x = (V^{\text{O}}, V^{\text{G}}, V^{\text{W}}, V^{\text{P}}, P^{\text{R}})$ (we will show that x is a possible state of the reservoir) and to the network controls u , giving

$$(F^{\text{O}}, F^{\text{G}}, F^{\text{W}}) = \Phi(x, u). \quad (16)$$

When considering only one well, a common assumption is that the production volumes are given by the Inflow Performance Relationship IPR, which is a function of the reservoir pressure P^R , the bottom-hole pressure P , the saturation of water S^W and the saturation of gas S^G . More precisely, we obtain, for a one well model, that

$$F_t^i = \Phi^i(x, u) = \frac{\text{IPR}^i(P_t^R - P_t, S_t^W, S_t^G)}{B_i(P_t^R)}, \quad \forall i \in \{\text{O}, \text{G}, \text{W}\}.$$

In the general case, we then need to take into account pressure drop due to the flow in the well itself through the use of a Vertical Lift Performance relationship.

In the two cases presented in Section 4, we can further detail the general production function Φ as follows

- For the gas reservoir as exposed in §4.1, we assume that the well only produces gas, and we hence obtain the following simplified formulation

$$F_t^G = \Phi^G(x, u) = \frac{\text{IPR}^G(P_t^R - P_t)}{B_G(P_t^R)}. \quad (17)$$

Indeed, when we only produce gas, there is no need to consider the different saturations. Those saturations are necessary to find the proportion of oil, water and gas produced when applying a difference of pressure $P^R - P$. Having only gas implies that the saturations have no impact on the production.

- When considering that the reservoir does not contain any free gas (i.e. $V^G = 0$ and $S^G = 0$), we obtain the following simplification for the production of oil and water. We assume that the *total production* F_t follows a simplified Darcy's law

$$F_t = \alpha(P_t^R - P_t), \quad \forall t \in \mathbb{T}, \quad (18)$$

where F_t is given by

$$F_t = F_t^O \times B_O(P_t^R) + \underbrace{F_t^G \times B_G(P_t^R)}_{=0} + F_t^W \times B_W(P_t^R), \quad (19)$$

with α the productivity index of the well, P_t the bottom-hole pressure of the well and F_t the total production which consists of a mix of oil and water as we have assumed that we have no free gas.

For the oil reservoir with water injection case presented in §4.2, the last assumption we make is that the amount of produced water is given by

$$F_t^W \times B_W(P_t^R) = \alpha(P_t^R - P_t) \text{WCT}(S_t^W), \quad (20)$$

where WCT is the water-cut function and, as already seen, where the water saturation is

$$S_t^W = \frac{V_t^W B_W(P_t^R)}{V_t^P}.$$

As we do not use more complex networks, we will not look any deeper into the network controls and their relationship with the general production Φ since those are beyond the scope of this paper.

A.4 Reservoir dynamics

We can now write the reservoir time evolution as a controlled dynamical system. The state of the controlled dynamical system is $x = (V^O, V^G, V^W, V^P, P^R)$. We also express the production volumes thanks to the general production function, Φ , defined in Equation (16).

Now, we show that using Equations (9), (10), (11), (13), (15) and (16) we can build a mapping f such that $x_{t+1} = f(x_t, u_t)$ for all $t \in \mathbb{T}$. We proceed as follows: we consider the conservation Equation (15)

at time $t + 1$, and use Equations (9), (10), (11) and (13) to obtain the equation

$$\begin{aligned} (V_t^o - F_t^o) \times B_o(P_{t+1}^R) + (V_t^w - F_t^w) \times B_w(P_{t+1}^R) \\ + \left[V_t^g - F_t^g + V_t^o \times (R_s(P_t^R) - R_s(P_{t+1}^R)) \right. \\ \left. + F_t^o \times R_s(P_{t+1}^R) \right] \times B_G(P_{t+1}^R) \\ = V_t^p (1 + c_f(P_{t+1}^R - P_t^R)) , \quad (21) \end{aligned}$$

which depends on the state and production volumes at time t and of the pressure of the reservoir at time $t + 1$. As recalled in §A.1, it is established in (Danesh, 1998, chap 2) that the left-hand side of Equation (21) is a decreasing function of the reservoir pressure P_{t+1}^R . More precisely, the expansion of the oil when gas dissolves into it due to an increase in pressure ΔP is less than the aggregated volume decrease of the free gas and the other fluids due to that same ΔP . To the contrary, the right-hand side of Equation (21) is increasing with the reservoir pressure. Hence, Equation (21) gives a function $\Xi : \mathbb{X} \times \mathbb{U} \rightarrow \mathbb{R}$ such that $\forall t \in \mathbb{T}, P_{t+1}^R = \Xi(x_t, u_t)$.

Moreover, note that when the PVT functions (B_o, B_G, B_w and R_s) are piecewise linear functions, the function Ξ can be computed efficiently. We only need to look at the breaking points of the piecewise linear functions to know on which segment we can invert Equation (21), thus getting the reservoir pressure P^R .

Combining Equations (9), (10), (11), (13) and using function Ξ , we finally obtain the expression of function f given in Equation (3).

B Material on state reduction

In this section, we detail how the general dynamics can be simplified in specific cases.

B.1 Gas reservoir state reduction

We consider a gas reservoir with no gas injection and where there is no water production or extraction, as used in §4.1, and we prove that the time evolution of the gas reservoir can be described by a reduced state composed of the standard volume of gas $x_t = V_t^G$.

By assumption, the reservoir contains only gas and a constant volume of water. Thus, the standard volume of water satisfies $V_t^w = V_0^w$ for all $t \in \mathbb{T}$ and the standard volume of oil satisfies $V_t^o = 0$ for all $t \in \mathbb{T}$. Hence, the state dimension can be reduced from dimension 5 to dimension 3.

Now, we show that the state dimension can be reduced to 1. First, we use Equation (12) in place of the linearized version (13) to obtain that $V_t^p = V_0 \exp(c_f P_t^R)$ for all $t \in \mathbb{T}$. Second, we consider Equation (15) at time t together with $V_t^o = 0$ and $V_t^w = V_0^w$ and $V_t^g = V_t^G - F_t^G$ to obtain

$$V_t^G \times B_G(P_t^R) + V_0^w \times B_w(P_t^R) = V_0 \exp(c_f P_t^R) , \quad \forall t \in \mathbb{T} . \quad (22)$$

The left-hand side of Equation (22) is a decreasing continuous function of the pressure (the volume of gas and the production being known) which we assume to be piecewise linear (we assume that the PVT functions are piecewise linear), whereas the right-hand side is an increasing and continuous function of the pressure. This implies that there can be at most one reservoir pressure which satisfies Equation (22). Moreover, since the left-hand side is piecewise linear, we can compute the reservoir pressure thanks to the \mathcal{W} Lambert function (the inverse relation of $f(w) = we^w$), and since pressure is positive, we use the \mathcal{W}_0 branch of the Lambert function. Finally, we obtain a function $\Psi : \mathbb{R} \rightarrow \mathbb{R}$ such that the pressure

$$P_t^R = \Psi(V_t^G) , \quad \forall t \in \mathbb{T} , \quad (23)$$

is the solution of Equation (22).

As the pressure, P_t^R , is given as a function of V_t^G and the pore volume, V_t^p , is given as a function of the pressure, P_t^R , we obtain a reduced state of dimension 1 given by the standard volume of gas V_t^G .

The only thing missing in order to get formulation (4) is to explicit the production function. The production of gas is given by Equation (17). As the reservoir pressure is given by the function Ψ , the production of gas when considering a one tank reservoir is given by

$$F_t^G = \frac{\text{IPR}^G(\Psi(V_t^G) - P)}{B_G(\Psi(V_t^G))} .$$

In the numerics, it is assumed that IPR^G , the inflow performance relationship of the well, is a piecewise linear function.

We consider two different models in §4.1: a one tank reservoir and a two tanks reservoir, as illustrated by Figure 2. In both cases, we have only one well and, as the optimization is done at the bottom of the well, the unique control is given by $u_t = P_t$. The state in the one tank case is $x_t = V_t^G$, whereas it is $x_t = ((V_t^G)^{(1)}, (V_t^G)^{(2)})$ for the two tanks case.

We denote by $\Psi_{1\mathbf{T}}$ the function which returns the reservoir pressure of the one tank case given a volume of gas in the reservoir (as defined in Equation (23)), and $\Psi_{2\mathbf{T}}$ the function for the producing tank pressure in the two tanks case.

The general production function $\Phi_{1\mathbf{T}}$ of the one tank case is hence given by

$$\Phi_{1\mathbf{T}}^G(x_t, u_t) = \frac{\text{IPR}^G(\Psi_{1\mathbf{T}}(x_t) - u_t)}{B_G(\Psi_{1\mathbf{T}}(x_t))} = F_t^G. \quad (24)$$

For the two tanks case, we consider that the well only produces gas from the first tank. The general production function $\Phi_{2\mathbf{T}}$ of the two tanks case is thus given by

$$\Phi_{2\mathbf{T}}^G(x_t, u_t) = \frac{\text{IPR}^G(\Psi_{2\mathbf{T}}^{(1)}(x_t) - u_t)}{B_G(\Psi_{2\mathbf{T}}^{(1)}(x_t))} = F_t^G. \quad (25)$$

In the Formulation (4) (for the one tank case), we split $\Phi_{1\mathbf{T}}^G$ in Constraints (4c) and (4d) to explicit the reservoir pressure and to mirror Equation (17).

Moreover, since we have only one well and since the IPR function is strictly monotonous, the production function of the well of Equation (4d) is injective. In the models considered here (one tank or two tanks), we can thus pass from the controls to the production and from the production to the controls without any ambiguity at a given state: the function $\Phi^G(x, \cdot)$ is a bijection, hence we find the (unique) bottom-hole pressure associated with a given production F^G when in state x . Finally, we obtain the admissibility set of the gas reservoir case. As the gas production F_t^G must be nonnegative, we obtain that the control must satisfy $P_t \in [0, P_t^R]$ for all time $t \in \mathbb{T}$, which gives the admissible control set

$$\mathcal{U}^{ad}(x_t) = [0, P_t^R] = [0, \Psi_{1\mathbf{T}}(x_t)]. \quad (26)$$

B.2 Oil reservoir with water injection state reduction

Now, we consider an oil reservoir where water injection is used to keep the reservoir pressure constant as in §4.2. To eliminate the possibility of having free gas in the reservoir, we assume that the initial pressure in the reservoir is above the bubble-point. Indeed, as we are going to keep the pressure constant, the pressure will always remain above the bubble-point.

We assume that the *produced water*² is given by Equation (20).

We now prove that the standard volume of water V_t^W may be used as a state for describing the reservoir dynamics. To start with, we have that $V_t^G = 0$, $F_t^G = 0$ and $P_t^R = P_0^R$ for all $t \in \mathbb{T}$. Moreover, using Equation (12) in place of the linearized version (13) we obtain that the pore volume is constant over time and given by $V_t^P = V_0 \exp(c_f P_0^R)$. Hence, the state dimension can be reduced from dimension 5 to dimension 2 as V_t^G , P_t^R and V_t^P are known over time.

Now, using Equation (15) combined with the fact that $V_t^G = 0$, we obtain that

$$V_t^O \times B_o(P_0^R) + V_t^W \times B_w(P_0^R) = V_0^P, \forall t \in \mathbb{T}. \quad (27)$$

Thus, the standard volume of oil in the reservoir is obtained as a function of the standard volume of water as follows

$$V_t^O = \frac{V_0^P - V_t^W \times B_w(P_0^R)}{B_o(P_0^R)}.$$

²Here, the produced water F^W is the water that is produced from the well. It should not be confused with the net produced water, which is the difference $F^W - F^{wi}$ between the water produced and the water injected

Moreover, using Equation (18) and Equation (20), for all time $t \in \mathbb{T}$, we have that

$$F_t^W = \Phi^W(V_t^W, P_t) \quad (28a)$$

$$\text{with } \Phi^W(V^W, P) = \frac{\alpha(P_0^R - P) \text{WCT}\left(\frac{V^W}{V_0^P} B_w(P_0^R)\right)}{B_w(P_0^R)}, \quad (28b)$$

and

$$F_t^O = \Phi^O(V_t^W, P_t) \quad (29a)$$

$$\text{with } \Phi^O(V^W, P) = \frac{\alpha(P_0^R - P) \left(1 - \text{WCT}\left(\frac{V^W}{V_0^P} B_w(P_0^R)\right)\right)}{B_o(P_0^R)}. \quad (29b)$$

Now, we turn to the time evolution of the standard volume of water. Equation (10) must be changed as we need to introduce the injected water F_t^{wi} at time t to obtain

$$V_{t+1}^W = V_t^W - F_t^W + F_t^{wi}, \quad \forall t \in \mathbb{T}. \quad (30)$$

It remains to show that the water injection can be deduced from the previous equations. Using Equation (15) at time $t + 1$ combined with Equation (30) and Equation (9) gives

$$(V_t^W - F_t^W + F_t^{wi}) \times B_w(P_0^R) + (V_t^O - F_t^O) \times B_o(P_0^R) = V_0^P, \quad (31)$$

which, using Equation (27), (28b) and (29b), gives

$$F_t^{wi} = F_t^W + F_t^O \times \frac{B_o(P_0^R)}{B_w(P_0^R)} = \frac{\alpha(P_0^R - P_t)}{B_w(P_0^R)}. \quad (32)$$

We conclude that we obtain a state dynamics with a one dimensional state $x_t = V_t^W$, a one dimensional control $u_t = P_t$, and state dynamics given by

$$V_{t+1}^W = V_t^W - \frac{\alpha(P_0^R - P_t) \left(\text{WCT}\left(\frac{V_t^W}{V_0^P} B_w(P_0^R)\right) - 1\right)}{B_w(P_0^R)}. \quad (33)$$

C Details on the impact of the states and controls discretizations

One tank gas reservoir. In the application of §4.1.1, we tried different discretization values for the state and control spaces. Results get better each time we increase the number of states or controls used in the loops of Algorithm 1. The optimal values and CPU times are compiled in Table 6. Discretization of the control space has less impact than discretization of the state space (there is no significant improvement when using more than 10 possible controls). We used 50 possible controls for the rest of the state discretization analysis to ensure we do not have any issues due to the control space. Moreover, the computation time grows linearly with the number of controls, hence we only got penalized by a factor of 5 for the computation time compared to being at the most efficient level for the discretization of the controls. We can also remark that going beyond 10,000 points for the state discretization yields no discernible improvement (less than 0.2%). However, the computation time grows exponentially with the state discretization. We hence used 10,000 points for the states and 20 controls for the results presented in §4.1.1.

Two tanks gas reservoir. We tried different discretization values for the two reservoirs problem of §4.1.2: 200×200 (i.e. the two reservoirs are discretized with 200 points each), 400×400 , 600×600 and $1,000 \times 1,000$. Results are summarized in Table 7, which shows the computation time of the optimization and the optimal value obtained. As can be seen, the computation time grows exponentially with the discretization, as we need to handle more and more values when we get a finer discretization. However,

State discretization	Value (M€)	CPU time (s)
100	602	1.25
200	689	1.45
500	725	2.50
1,000	736	7.50
2,000	740	25.20
5,000	742	110.00
10,000	743	653.00
20,000	743	2,288.00
50,000	743	8,142.00

Table 6: Summary of the impact of the discretization of the state space on the one tank formulation, with 50 possible controls

performance remains reasonable for the number of time steps considered. We can also remark that going past a 200×200 discretization of the states of the reservoir does not improve the optimal value. A very small impact is observed from the discretization of the controls. Indeed, almost no improvement is obtained above 10 possible controls (we hence used 50 possible controls in Table 7 to ensure the discretization of the controls will not influence the analysis of the discretization of the states). All the results of §4.1.2 were therefore computed with the 400×400 discretization for the states, and 20 for the controls.

State discretization	CPU time (s)	Value (M€)
50×50	5.1	730
100×100	28.3	735
200×200	115.3	736
400×400	706.0	736
600×600	3,893.0	736
1000×1000	18,089.0	736

Table 7: Impact of the discretization of the state space on the two tanks model, with 50 possible controls

Oil reservoir with water injection. We tried different values for the discretization of the state space of the problem described in §4.2. However, the discretization of the controls had no impact, as the controls only took two different values: either no production, or production at the maximal rate. We therefore chose 10 possible controls to ensure we do not missed another behavior during the analysis on the impact of the discretization of the states. Table 8 compiles the time to solve and the associated results of the optimization depending on the number of points considered for the discretization of the states space. We note that there is not a lot of gain from going from 10,000 points to 100,000 points in the discretization, whereas computation time grows by more than 100 times.

Discretization	Time steps	CPU time (s)	Value (M€)
1,000	240	0.35	3182
10,000	240	12.05	3358
100,000	240	1575	3376

Table 8: Summary of the dynamic programming results for the oil reservoir with water injection

D Additional material on the decline curves formulation

Usually, formulations using decline curves, as can be seen in the works of [Iyer et al. \(1998\)](#), are of the form:

$$\max_u \sum_{t=0}^T \rho^t \mathcal{L}_t(u_t) \quad (34a)$$

$$s.t. \quad F_t^o \leq h \left(\sum_{s=0}^{t-1} F_s^o \right), \quad \forall t \in \mathbb{T} \setminus \{0\}, \quad (34b)$$

$$u_t \in \mathcal{U}_t^{ad} \left(\sum_{s=0}^{t-1} F_s^o \right), \quad \forall t \in \mathbb{T}. \quad (34c)$$

Using decline curves, or oil deliverability curves, means using Equation (34b) to predict the reservoir's behavior. It states that the maximal rate at time t only depends on the oil cumulated production until time t . In the general case, there is no reason to believe that there is an equivalence between a material balance model for the reservoir and a decline curve represented with a function h .

However, when the state of the material balance formulation can be reduced to a one dimensional state (such as a reservoir which only contains gas), there can be an equivalence between the decline curve and the material balance formulations, as was stated in Proposition 3.

Proof of Proposition 3. Let us consider the component $\Phi^G : \mathbb{X} \times \mathbb{U} \rightarrow \mathbb{R}$ of the production mapping $\Phi : \mathbb{X} \times \mathbb{U} \rightarrow \mathbb{R}^3$ such that

$$F_t^G = \Phi^G(x_t, u_t). \quad (35)$$

Therefore, we have

$$F_t^G \leq \max_u \Phi^G(x_t, u). \quad (36)$$

Moreover, having a one-dimensional state greatly simplifies the dynamics, as we only need to consider one fluid. The dynamics thus simplifies to

$$x_{t+1} = f(x_t, u_t) = x_t - F_t^G. \quad (37)$$

By propagating the simplified dynamics (37) and by re-injecting it in Equation (36), we get:

$$F_t^G \leq \max_u \underbrace{\Phi^G \left(x_0 - \sum_{s=0}^{t-1} F_s^G, u \right)}_{h(\sum_{s=0}^{t-1} F_s^G)}. \quad (38)$$

Hence, Equation (38) defines the function h . The equivalence exists when the state is reduced to one dimension (as similar reasoning can be applied to the other one-dimensional cases). \square

However, when considering more complex cases, such as a reservoir with both oil and gas, or when there is water encroachment (influx of water in the reservoir from the aquifer), we cannot have a reduction to a one-dimensional state. Decline curves, or oil deliverability curves, will not be equivalent to the material balance system, as they can only represent a one dimensional dynamical system, where the state is the cumulated production.

Even if we have a state that cannot be reduced to one dimension, we can still propagate the dynamics in Equation (35):

$$\begin{aligned} F_t^G &= \Phi^G(x_t, u_t) \\ &= \Phi^G(f(f(\dots f(x_0, u_0), \dots), u_{t-1}), u_t). \end{aligned}$$

However, there is no reason to believe that there exists a function h depending on the sum of productions in the general case, contrarily to the one-dimensional case. This is why those functions are generated with a given production planning, i.e. a series of controls applied to the reservoir. Given a series of admissible controls $\tilde{\mathbf{U}} = (\tilde{u}_0, \dots, \tilde{u}_T)$, one can create an oil-deliverability curve, that takes as argument

Algorithm 2: Finding the points of the piecewise linear function $\tilde{h}_{\tilde{\mathbf{U}}}$

```
control_to_apply =  $\tilde{\mathbf{U}}$ ;
current_state =  $x_0$ ;
cumulated_production = 0;
max_production =  $\max_u \Phi^G(\text{current\_state}, u)$ ;
list_of_points = {(cumulated_production, max_production)};
for  $t$  from 1 to  $T$  do
     $\tilde{u} = \text{control\_to\_apply}[t]$ ;
    production =  $\Phi^G(\text{current\_state}, \tilde{u})$ ;
    cumulated_production = cumulated_production + production;
    current_state =  $f(\text{current\_state}, \tilde{u})$ ;
    max_production =  $\max_u \Phi^G(\text{current\_state}, u)$ ;
    push(list_of_points, (cumulated_production, max_production));
end
return  $\text{list\_of\_points}$ 
```

the total cumulated production and returns the maximal possible production. It however depends on the underlying production planning $\tilde{\mathbf{U}}$. We can create such function $\tilde{h}_{\tilde{\mathbf{U}}}$ through the Algorithm 2.

Once we have a list of points of $\tilde{h}_{\tilde{\mathbf{U}}}$, we consider a linear interpolation between those points as the decline curve we use in the optimization problem (5).

In (Iyer et al., 1998; Marmier et al., 2019), the authors use decline curves, i.e. oil-deliverability curves with natural depletion at the maximal rate. This means that there is no injection, and the production planning consists of maximal production rates. We can generate those decline curves with a tweaked version of the previous procedure (see Algorithm 3).

Algorithm 3: Finding the points of the piecewise linear function h

```
current_state =  $x_0$ ;
cumulated_production = 0;
max_production =  $\max_u \Phi^G(\text{current\_state}, u)$ ;
list_of_points = {(cumulated_production, max_production)};
for  $t$  from 1 to  $T$  do
     $\tilde{u} = \arg \max_u \Phi^G(\text{current\_state}, u)$ ;
    production =  $\Phi^G(\text{current\_state}, \tilde{u})$ ;
    cumulated_production = cumulated_production + production;
    current_state =  $f(\text{current\_state}, \tilde{u})$ ;
    max_production =  $\max_u \Phi^G(\text{current\_state}, u)$ ;
    push(list_of_points, (cumulated_production, max_production));
end
return  $\text{list\_of\_points}$ 
```

References

- D. P. Bertsekas. *Dynamic programming and optimal control. Vol. 1.* Athena Scientific, Belmont, Mass, 4th edition, 2016.
- J. M. Bohannon. A Linear Programming Model for Optimum Development of Multi-Reservoir Pipeline Systems. *Journal of Petroleum Technology*, 22(11):1429–1436, Nov. 1970. doi: 10.2118/2626-PA.
- J. A. Caballero and I. E. Grossmann. An algorithm for the use of surrogate models in modular flowsheet optimization. *AIChE Journal*, 54(10):2633–2650, Oct. 2008. doi: 10.1002/aic.11579.
- E. Camponogara, A. F. Teixeira, E. O. Hulse, T. L. Silva, S. Sunjerga, and L. K. Miyatake. Integrated Methodology for Production Optimization from Multiple Offshore Reservoirs in the Santos Basin.

- IEEE Transactions on Automation Science and Engineering*, 14(2):669–680, Apr. 2017. doi: 10.1109/TASE.2016.2640240.
- L. Dake. *Fundamentals of Reservoir Engineering*. Elsevier Science, 1983.
- A. Danesh. *PVT and Phase Behaviour Of Petroleum Reservoir Fluids*. Elsevier Science, 1998.
- A. Davis. Optimal field development and production design for unconventional reservoirs: A case study from Central Sub-Basin, Permian Basin, New Mexico. *Petroleum Research*, page 11, 2021.
- E. I. Epelle and D. I. Gerogiorgis. A computational performance comparison of MILP vs. MINLP formulations for oil production optimisation. *Computers & Chemical Engineering*, 140:106903, Sept. 2020. doi: 10.1016/j.compchemeng.2020.106903.
- L. Frair and M. Devine. Economic Optimization of Offshore Petroleum Development. *Management Science*, 21(12):1370–1379, Aug. 1975. doi: 10.1287/mnsc.21.12.1370.
- D. I. Gerogiorgis, M. Georgiadis, G. Bowen, C. C. Pantelides, and E. N. Pistikopoulos. Dynamic oil and gas production optimization via explicit reservoir simulation. In W. Marquardt and C. Pantelides, editors, *Computer Aided Chemical Engineering*, volume 21 of *16th European Symposium on Computer Aided Process Engineering and 9th International Symposium on Process Systems Engineering*, pages 179–184. Elsevier, Jan. 2006. doi: 10.1016/S1570-7946(06)80043-X.
- V. Gupta and I. E. Grossmann. An efficient multiperiod MINLP model for optimal planning of offshore oil and gas field infrastructure. *Industrial & Engineering Chemistry Research*, 51(19):6823–6840, 2012. doi: 10.1021/ie202959w.
- V. Gupta and I. E. Grossmann. Multistage stochastic programming approach for offshore oilfield infrastructure planning under production sharing agreements and endogenous uncertainties. *Journal of Petroleum Science and Engineering*, 124:180 – 197, 2014. doi: 10.1016/j.petrol.2014.10.006.
- G. Hegguler, S. Barua, and W. Bard. Integration of a Field Surface and Production Network With a Reservoir Simulator. *SPE Computer Applications*, 9(03):88–92, May 1997. doi: 10.2118/38937-PA. Publisher: OnePetro.
- B. Hong, X. Li, S. Song, S. Chen, C. Zhao, and J. Gong. Optimal planning and modular infrastructure dynamic allocation for shale gas production. *Applied Energy*, 261:114439, Mar. 2020. doi: 10.1016/j.apenergy.2019.114439.
- R. R. Iyer, I. E. Grossmann, S. Vasantharajan, and A. S. Cullick. Optimal planning and scheduling of offshore oil field infrastructure investment and operations. *Industrial & Engineering Chemistry Research*, 37(4):1380–1397, 1998. doi: 10.1021/ie970532x.
- C. S. Khor, A. Elkamel, and N. Shah. Optimization methods for petroleum fields development and production systems: a review. *Optimization and Engineering*, 18(4):907–941, Dec. 2017. doi: 10.1007/s11081-017-9365-2.
- G. Lei, T. L. Silva, and M. Stanko. Compact formulations for efficient early-phase field development optimization of multi-reservoir fields. *Computers & Chemical Engineering*, 150:107319, July 2021. doi: 10.1016/j.compchemeng.2021.107319.
- G. Lei, M. Stanko, and T. L. Silva. Formulations for automatic optimization of decommissioning timing in offshore oil and gas field development planning. *Computers & Chemical Engineering*, 165:107910, Sept. 2022. doi: 10.1016/j.compchemeng.2022.107910.
- R. Marmier, U. Awasthi, and I. E. Grossmann. Multiperiod optimization model for oilfield production planning: bicriterion optimization and two-stage stochastic programming model. *Optimization and Engineering*, 07 2019. doi: 10.1007/s11081-019-09455-0.
- A. Moolya, A. Rodríguez-Martínez, and I. E. Grossmann. Optimal producer well placement and multiperiod production scheduling using surrogate modeling. *Computers & Chemical Engineering*, 165: 107941, Sept. 2022. doi: 10.1016/j.compchemeng.2022.107941.

- P. Sarma, L. J. Dzzurlofsky, K. Aziz, and W. H. Chen. Efficient real-time reservoir management using adjoint-based optimal control and model updating. *Computational Geosciences*, 10(1):3–36, Mar. 2006. doi: 10.1007/s10596-005-9009-z.
- A. Satter and G. M. Iqbal. 13 - decline curve analysis for conventional and unconventional reservoirs. In A. Satter and G. M. Iqbal, editors, *Reservoir Engineering*, pages 211–232. Gulf Professional Publishing, Boston, 2016. doi: 10.1016/B978-0-12-800219-3.00013-9.
- L. Silva and C. Guedes Soares. Oilfield development system optimization under reservoir production uncertainty. *Ocean Engineering*, 225:108758, Apr. 2021. doi: 10.1016/j.oceaneng.2021.108758.